Cooling Fan Model for the Thermal Design of Compact Electronic Equipment—Modeling of Swirl Flow at the Exit of an Axial Flow Fan

Hajime Nakamura
Department of Mechanical Engineering, National Defense Academy of Japan, Yokosuka, Japan.
Email: nhajime@nda.ac.jp

***Abstract*—To hasten the thermal design for forced convection electronic devices, cooling fans should be modeled to reduce a computational load. A fan curve model, which generates the volumetric flow rate according to the PQ curve, is very simple and usually incorporated into commercial CFD (computational fluid dynamics) codes. However, the conventional model does not specify the flow field at the exit of a fan since the PQ curve has no information on the swirl flow. Thus, in this work, the swirl force acting on the flow was modeled mathematically by introducing a non-dimensional "swirl coefficient," which can be incorporated into the fan curve model. The swirl coefficient was evaluated using a detailed CFD simulation, which takes the rotating blades into account, and the result indicates that this coefficient can be treated as a constant regardless of the radial position of the blade. Subsequently, the flow behind the fan was simulated using the fan curve model incorporated with the swirl coefficient. As a result, it was confirmed that a realistic velocity distribution could be generated within the normal usable range of the fan where the rotating stall does not occur.**

***Index Terms*—Axial flow fan, modeling, PQ curve, swirl flow, thermal design, electronic equipment**

I. Introduction

In general, a fan curve model is incorporated into the commercial CFD (computational fluid dynamics) codes used for the thermal design of electronic devices. This model generates a flow rate versus pressure difference between the front and rear of the fan according to the PQ curve [1], [2]. The merit of this model is to reduce the computational load since it is not necessary to calculate the flow around the rotating blades. However, some studies have reported that this model often generates erroneous results (e.g., [3]). The preliminary examination performed during the RC227 research project (2006.4-2008.3) of the Japan Society of Mechanical Engineers (JSME) indicated that reasonable results are not obtained due to the following three reasons.

1) The difference in the pressure definition of the fan curve model from the PQ curve.

2) The change in the fan performance due to the flow obstruction observed in close proximity to the fan.

3) An inaccurate swirl velocity at the exit of the fan.

Problem 1) can be easily solved by correcting the pressure definition of the PQ curve, as presented in the literature [1], [4]. In this paper, the solution to problem 3), that is, how to generate a realistic swirl flow using the fan curve model, was examined. As for problem 2), several studies (e.g., [5] and [6]) have been conducted to date.

II. Basic Idea to Generate Realistic Swirl Flow

In the existing CFD codes, the swirl flow of the fan curve model can often be simulated by giving the swirl ratio (swirl velocity divided by the axial velocity) (e.g., [7]) or the angular velocity ratio (flow angular velocity divided by the impeller rotation angular velocity) (e.g., [8]) at the fan exit. However, it is difficult to estimate these values from the information that the user can easily obtain, especially for small fans used in electronic devices. Furthermore, whether these methods are physically valid does not seem to have been properly verified. Therefore, in this work, a general and simple method was developed to generate the swirl flow based on fluid dynamics.

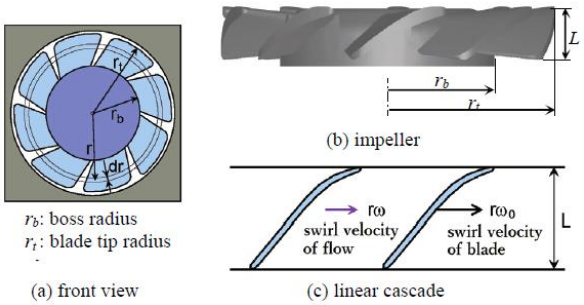

Figure 1. A schematic of an axial flow fan.

A. Definition of the Swirl Coefficient

Fig. 1 shows a schematic of an axial flow fan. The rotation of the impeller acts as a swirling force to the flow. This force F_θ can be given by the following equation.

$$F_\theta = n \int_{r_b}^{r_t} C_\theta (0.5\rho)(r\omega_0 - r\omega)^2 L\, dr \qquad (1)$$

where n is number of blades attached to the impeller, L is the axial length of the blade (see Fig. 1 (b)), ρ is the density of air, ω_0 is rotational angular velocity of the

Manuscript received September 1, 2017; revised December 12, 2017.

doi: 10.18178/ijeetc.7.1.21-25

blade, ω is angular velocity of fluid and r_b and r_t are the radius of the boss and the blade tip, respectively. The value of $r(\omega_0–\omega)$ represents the relative swirl velocity of the blade to the flow and the integral "$\int Ldr$" represents the projected area of the blade to the flow. Thus, C_θ is a dimensionless coefficient similar to the drag and lift coefficients in fluid dynamics. Herein, we call C_θ the "swirl coefficient." This coefficient can be regarded as a constant if the flow field around the blades is similar. That is, if the geometry of the blade is similar, the swirl coefficient C_θ can be regarded as a constant regardless of the dimension and the rotation speed of the blade as long as a rotating stall does not occur.

B. *Evaluation of the Swirl Coefficient Using a Detailed CFD Simulation*

First, a detailed CFD simulation was performed to evaluate the swirl coefficient using the CAD (computer aided design) data of a small axial flow fan with a square side length of 40 mm and axial length of 10 mm (this dimension is referred to as □40×10 hereinafter), which consists of an impeller and frame, as shown in Fig. 2 (a). The computations were carried out using the unstructured grid system in SCRTU/Tetra of CRADLE. A sufficiently wide space was provided in front of and behind the fan, as shown in Fig. 2, and a uniform static pressure was applied to the inlet and exit of the computational domain, corresponding to the measurement of the PQ curve [4]. Fig. 2 (b) shows the calculation grid at the center cross-section. The impeller was rotated at an angular velocity corresponding to the measurement using the function provided in the CFD software. The SST k-ε model was used as a turbulence model. The thickness of the first mesh on the blade and its surrounding wall surface was set to y^+ <2. The total number of volume elements was about 2.4 million. The calculation was performed by systematically changing the pressure difference ΔP between the inlet and exit of the computational domain.

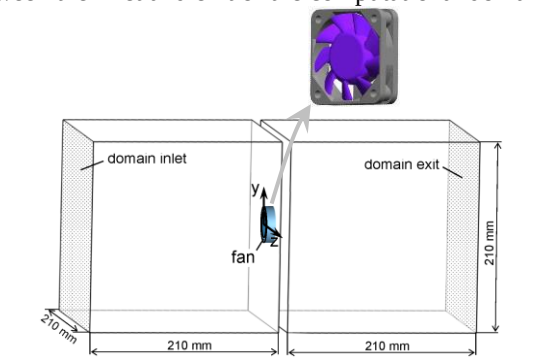

(a) Computational domain

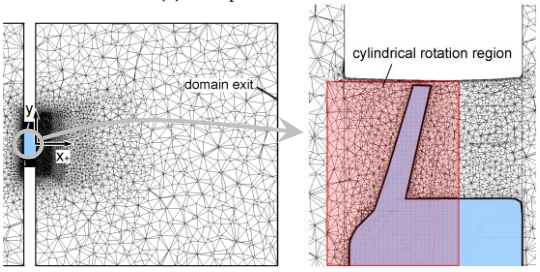

(b) Grid at the center cross-section (x-y plane, z = 0)

Figure 2. The CFD simulation considering the actual shape of the fan.

Fig. 3 shows the generated flow rate Q versus pressure difference ΔP between the inlet and exit of the computational domain, which was compared with the PQ curve obtained experimentally [4]. The simulation was carried out with and without the turbulence model, and the results showed that the difference between them was small. The calculated flow rate reasonably agreed with the experimental data over the conditions studied, as shown in Fig. 3, including at a higher pressure difference in which the flow around the rotating blades separated. The flow rate was somewhat smaller at a lower pressure difference, which is likely to originate from the fact that the geometry of the blade used in the CAD data was not completely consistent with that used in the experiment. Fig. 4 shows a comparison of the velocity distribution behind the fan with free air flow (ΔP = 0, top figures) and at ΔP = 12 Pa (bottom figures) at the center cross-section (x-y plane, z = 0). The left figures show the axial velocity u_x and the right figures show the swirl velocity u_z. The sign of u_z is reversed up and down since it was plotted as the velocity along the z direction. The data measured using laser Doppler velocimetry (LDV) was plotted as solid dots. The distributions of both the axial and the swirl velocities at the exit of the fan (x_+ = 1 mm; 1 mm downstream from the discharge side of the fan) agrees well with the measured data. This indicates that the fluid flow generated by the rotation of the impeller was appropriately calculated using this simulation.

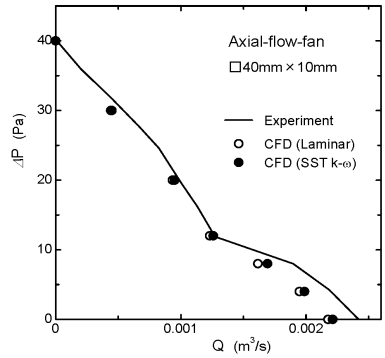

Figure 3. A comparison of the PQ curve.

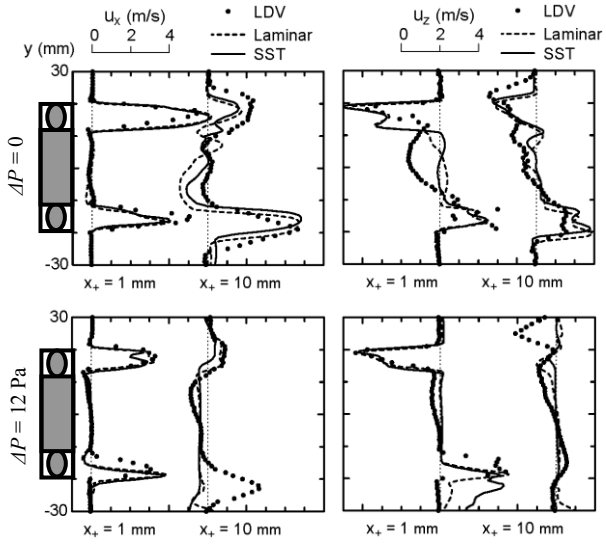

Figure 4. The velocity distribution behind the fan at z = 0.

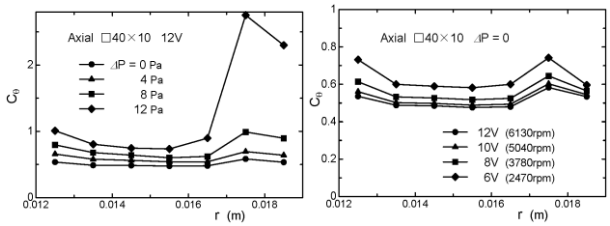

(a) The effect of pressure difference (b) The effect of the rotation speed

Figure 5. The swirl coefficient C_θ.

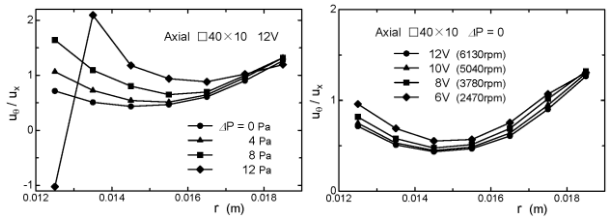

(a) The effect of the pressure difference (b) The effect of the rotation speed

Figure 6. The swirl ratio u_θ/u_x.

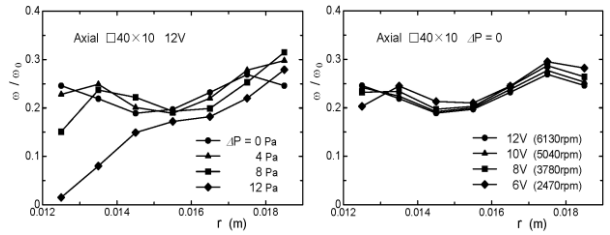

(a) The effect of the pressure difference (b) The effect of the rotation speed

Figure 7. The angular velocity ratio ω/ω_0.

Then, the swirl coefficient C_θ acting on each radial position of the blade was evaluated from the computational results, as shown in Fig. 5. The value of C_θ does not change significantly even if the pressure difference ΔP and the rotation speed of the impeller changes, as long as a rotating stall does not occur (at $\Delta P \leq 8$ Pa for this fan). That is, within the normal usable range, it is considered to be reasonable to treat C_θ as a constant (about 0.6 in this case). For comparison, the swirl ratio u_θ/u_x and the angular velocity ratio ω/ω_0 at the exit of the fan are also presented in Fig. 6 and Fig. 7, respectively. In both cases, the value falls within a certain range as long as a rotating stall does not occur. However, especially for the swirl ratio, the change in its value is large compared with the swirl coefficient, so it is better not to treat this as a constant.

III. CFD Simulation Using The Fan Curve Model

Next, a CFD simulation was performed using the fan curve model incorporating the swirl coefficient.

A. Computational Method

Fig. 8 shows the computational domain and grid. A sufficiently wide space was provided in front of and behind the fan, and a uniform static pressure was applied to the inlet and exit of the computational domain as well as the detailed simulation. Fan blowing was expressed by the fan curve model based on the PQ curve in the same manner as presented in Ref. [4]. In addition, the swirl force was generated using Eq. (1) with the swirl coefficient C_θ = 0.6. In this case, the geometry of the rotating blades is not necessary and the fan can be basically represented using a double cylinder, as shown in Fig. 8 (a), so the mesh number can be greatly reduced. Herein, the computation was performed using two geometries (see the illustration at the top of Fig. 8 (a)): One is represented using only a double cylinder whose inner cylinder corresponds to the boss and outer cylinder corresponds to the frame, and the other considers the supports, which connect the boss to the frame. Hennissen *et al*. [7] pointed out from their LDV measurements that the existence of the supports greatly affects the velocity distribution at the exit of the fan. The number of volume elements was about 160,000 for the double cylinder and about 220,000 for the case where the supports were considered. The mesh numbers were less than one-tenth of the detailed simulation.

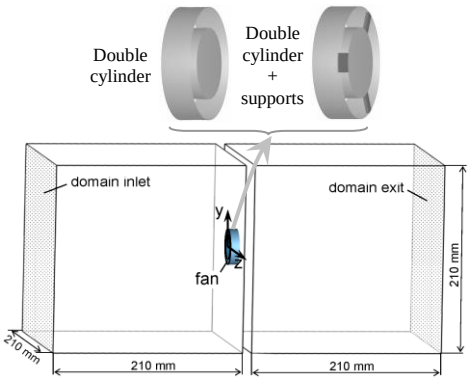

(a) Computational domain

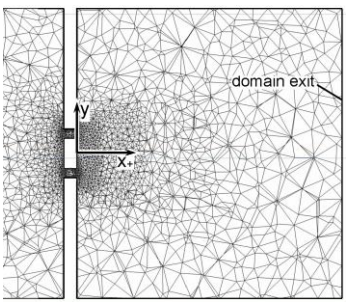

(b) Grid at the center cross-section (x-y plane, z = 0)

Figure 8. The CFD simulation using the fan curve model.

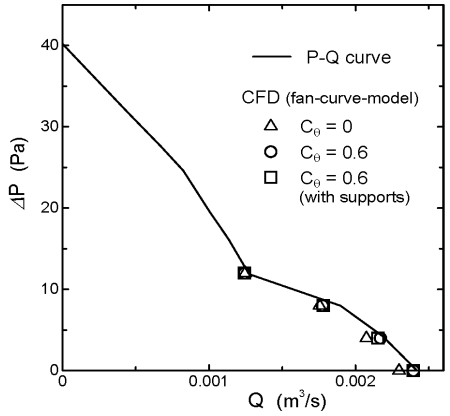

Figure 9. A comparison of the volumetric flow rate.

B. Results

Herein, the following three calculations were performed: 1) A calculation without the swirl force (C_θ = 0) using a double cylinder, 2) a calculation considering the swirl force (C_θ = 0.6) using a double cylinder and 3) a calculation considering the swirl force (C_θ = 0.6) using a double cylinder with supports. Fig. 9 shows a plot of the volumetric flow rate Q obtained using these calculations with respect to the pressure difference ΔP. In any condition, that is, whether the swirl force was applied, and whether the supports were considered or not, the flow rate was in good agreement with the measured value (denoted by a solid line in Fig. 9).

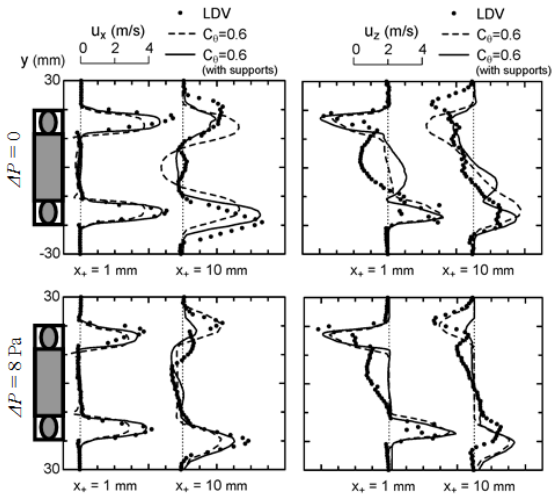

Figure 10. The velocity distribution behind the fan at z = 0.

Fig. 10 shows a comparison of the velocity distribution behind the fan. The distributions of the axial velocity u_x and the swirl velocity u_z at x_+ = 1 mm from the fan discharge side are in good agreement with the measured data considering the swirl force (C_θ = 0.6) for both cases with free air flow (ΔP = 0, top figures) and a large pressure difference (ΔP = 8 Pa, bottom figures). In particular, the consideration of the supports, which obstruct the flow, results in a closer distribution to the measured data.

Fig. 11 shows the contour of the axial velocity u_x in the xy cross-section at the center of the fan (z = 0). If the swirl force is not considered (Fig. 11 (b), C_θ = 0), the discharged flow is sucked into the inner region where the pressure is low. In contrast, by considering the swirl force (Fig. 11 (c), C_θ = 0.6), the direction of the discharged flow is shifted outward due to the centrifugal force produced by the swirl flow and approaches the measured data (Fig. 11 (a)). Moreover, by considering the supports (Fig. 11 (d)), the obstruction of the flow makes the distribution closer to the measured data.

The generality of this model was investigated using other axial-flow-fans with different dimensions (□80×25, □60×25, □20×10 and □17×8) [9], [10]. As a result, it was confirmed that a reasonable velocity distribution can be generated using a swirl coefficient of C_θ = 0.6 for the fans from □40 to □80. In contrast, for the ultra-small fans of about □20, the value of C_θ increased to about 1 probably due to the low-Reynolds-number effect.

Incidentally, the fan curve model proposed herein can be applied even when the flow around the fan is obstructed as long as the performance of the fan itself does not change. Only the condition where the flow obstruction changes the angle of attack of the flow around the blade degrades the fan performance [11]. This situation is likely to be caused when the flow at the upstream side of the fan is highly obstructed. For example, in the case when a solid flat plate is placed close to the suction side of the fan (□40×10), the fan performance degrades at a gap of <12 mm [12]. In this condition, it is necessary to perform a detailed simulation taking the geometry of the rotating blades into account [13], [14] or to develop a new fan model that considers the change in the performance of the fan by flow obstruction.

IV. Conclusions

In this paper, a general method to generate a reasonable swirl flow behind an axial flow fan was proposed using the fan curve model. The swirl flow was modeled based on the swirl force acting on the flow upon the rotation of the blades. As a result, the following was clarified.

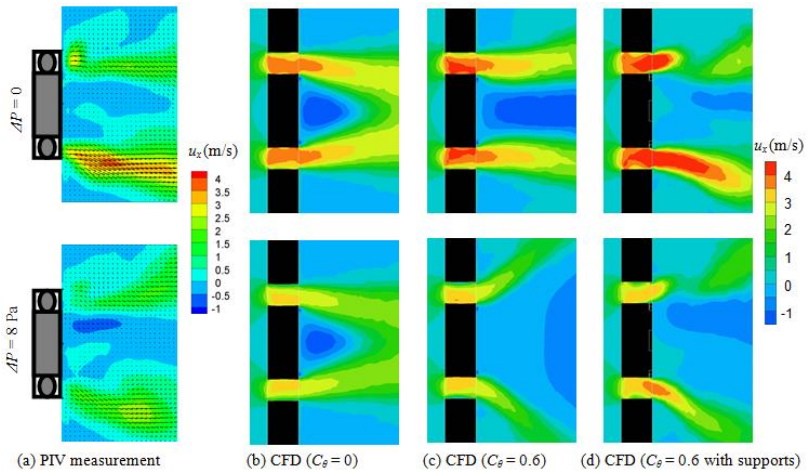

Figure 11. The contour of the axial velocity u_x at the center cross-section (x-y plane, z = 0).

1) The swirl coefficient C_θ in Eq. (1) can be treated as a constant (C_θ = 0.6 for the fan examined in this study) within the normal usable range where a rotating stall does not occur.

2) It was confirmed that the fan curve model considering the swirl coefficient C_θ generates a reasonable velocity distribution behind the fan when compared to the measured data. In particular, the consideration of the supports that connect the boss to the frame made the velocity distribution closer to the measured data.

ACKNOWLEDGMENT

This study was performed as a part of the RC239 research project (2008.4-2010.3) of the Japan Society of Mechanical Engineers (JSME). The author wishes to express his gratitude to all the members of the working group for their helpful discussions. The author also wishes to acknowledge the former students of the National Defense Academy of Japan, for their assistance in conducting the experiments.

REFERENCES

[1] W. Temmerman, F. Christiaens, and M. Baelmans, "Application of fan models for thermal simulation," in *Proc. ISPS '97*, 1997, pp. 81-86.

[2] J. Stein and M. M. Hydeman, "Development and testing of the characteristic curve fan model," *ASHRAE Transactions*, vol. 110, pp. 347-356, 2004.

[3] R. Grimes, M. Davies, J. Punch, T. Dalton, and R. Cole, "Modeling electronic cooling axial fan flows," *Trans. ASME, J. Electronic Packaging*, vol. 123, pp. 112-119, 2001.

[4] H. Nakamura, "Cooling fan model for thermal design of compact electronic equipment (Improvement of modeling using PQ curve)," in *Proc. ASME 2009 InterPACK Conf.*, InterPACK2009-89010, 2009.

[5] H. Nakamura, T, Fukue, K. Koizumi, and M. Ishizuka, "Reduction in flow rate of small cooling fans by an obstruction," *Trans. Japan Soc. Mech. Eng., Ser. B*, vol. 76-768, pp. 1184-1190, 2010. (in Japanese)

[6] T. Fukue, M. Ishizuka, T. Hatakeyama, A. Nakagawa, and K. Koizumi, "Study on P-Q curves of cooling fans for thermal design of electronic equipment (Effects of opening position of obstructions near a fan)," in *Proc. ASME-JSME-KSME Joint Fluids. Eng. Conf.*, AJK2011-22054, 2011.

[7] J. Hennissen, W. Temmerman, J. Berghmans, and K, Allaert, "Modelling of axial fans for electronic equipment," in *Thermal Management of Electronic Systems II*, E. Beyne, *et al*., Eds., Kluwer Academic Publishers, 1997, pp. 309-318.

[8] Application examples of software cradle (2014). [Online]. Available: http://www.cradle-cfd.com/casestudy/user_interview/0000000011

[9] H. Nakamura, "Cooling fan model for thermal design of electronic equipment (Modeling of an axial-flow-fan using non-dimensional swirling coefficient," in *Proc. 48th National Heat Transfer Symposium of Japan*, F134 (in Japanese), 2011.

[10] H. Nakamura, "Modeling of axial-flow-fan using non-dimensional swirling coefficient (A case of ultra-small fans of about □20," in *Rep. RC256 Research Project of Japan Soc. Mech. Eng.*, 2014, pp. 551-559. (in Japanese)

[11] H. Metwally. (2006). Increasing air cooling efficiency through advanced fan modeling. ANSYS paper, WP114. [Online]. Available:https://support.ansys.com/staticassets/ANSYS/staticassets/resourcelibrary/whitepaper/fan-modeling-wp114.pdf

[12] H. Nakamura, "Modeling of an axial-flow-fan using non-dimensional swirl coefficient (Effect of an obstruction)," in *Proc. 49th National Heat Transfer Symposium of Japan*, C324, 2012. (in Japanese).

[13] A. Sahili, B. Zogheib, and R. M. Barron, "3-D Modeling of Axial Fans," *Applied Mathematics*, vol. 4, pp. 632-651, 2013.

[14] K. Koizumi, T. Hatakeyama, T. Fukue, and M. Ishizuka, "MRF modeling of axial fan for thermal simulation of electronic equipment," *Trans. Japan Institute of Electronic Packaging*, vol. 7, no. 1, 2014.

Hajime Nakamura received his B.E. degree in Mechanical Engineering from the Tokyo Institute of Technology and M.E. and D.E. degrees in Energy Science from the Tokyo Institute of Technology. His research mainly focuses on convective heat transfer in turbulent flows with flow separation and reattachment. Also, his fields of interest include flow control around bluff bodies and the thermal design of heat transfer devices.

He is a Professor of Thermal Engineering Laboratory in the Department of Mechanical Engineering at the National Defense Academy of Japan. An outline of the research and activities of the Nakamura laboratory is available at http://www.nda.ac.jp/~nhajime/english/index.html

Prof. Nakamura belongs to the Japan Society of Mechanical Engineers (JSME), the Heat Transfer Society of Japan, the Japan Society of Fluid Mechanics and the Visualization Society of Japan.